Contents

Chapter 1

Reconstruction of Physics Object

To allow the use of all the information enclosed in a bunch crossing, the collection of all ATLAS detector signals needs to be translated in more user friendly object, the reconstruction of the event is carryed out by the ATLAS event reconstruction software framework ATHENA [45].

Physical particle like electron, muons, hadronic jets, ecc, are all described by means of off line software reconstructed object. In section **??** the electron reconstuction algorithm is briefly described, for more details on reconstructed object and their performance see [53]

1.1 Tracks and Vertex Reconstruction

The reconstruction of charged particles tracks and interaction vertex is based on Inner Detector information, charged particle bends in the transverse plane due to the magnetic field of the Inner Detector and this allow to measure their transverse momentum, they can only be reconstructed whithin $|\eta| < 2.5$. To fully carachterize a track other parameters need to be measured and those are: the ϕ and θ angles to define its direction, the impact parameter is the distance of clostest approach o the track to the beam axis calculated with respect to the origin of coordinate, d_0 is the impact parameter in the $x - y$ plane, while z_0 is along the z axis. The transverse impact parameter d_0 is the distance of closest approach of the track to the primary vertex point in the $r - \phi$ projection. The z coordinate of the track at this point of closest approach is referred to z_0

Track Reconstruction Tracks are reconstructed by the Inner Detector track reconstruction software [48]. First raw data from the pixel and SCT detectors are transformed in three dimensional space points which are called "hits", while the TRT detector information is translated into drift circles. Thn, track seeds are formed from a combination of space-points in the three pixel layers and the first SCT layer, these seeds are then extended throughout the SCT to form track candidates. The tracks candidate are fitted using a *Kalman filter* algorothm [49], ambiguities in the cluster-to-track association are resolved and fake tracks are rejected. The selected tracks are then extended to the TRT and finally refitted with the full information of all three detectors. To help improve tracking efficiency for secondary tracks coming from photon conversion or decays of long-lived particles (like kaons), a complementary algorithm searches foir unused track segments in the TRT, which will be then extended towards the SCT and the pixel in a very similar way as described for the default algorithm. All tracks found with $P_T > 100$ MeV are written to the database.

Vertex Reconstruction The vertex recostruction algorithm and its performance are described in full detail in [53, 52] and only briefly summarized here. The vertex finding is perfomed as follows: a set of well reconstructed tracks are selected, a vertex is seeded according to the global maximum of the selected tracks z coordinate distribution, the tracks z coordinate is computed with respect the expected averange collision point. An adaptive vertex fitting algorithm [51] determines the vertex position taking as input the vertex seed position and the tracks around it. Tracks that are incompatible with the found vertex by more than seven standard deviation are used to seed the next vertex. The iteration continues untill no tracks are left or no additional vertex can be found. The procedure depends on the expected position of the averange interaction point, which is monitored during LHC data taking and is computed every few minutes with the method described in [50].

The vertex with the larger sum of tracks P_T associated is identified as the *primary vertex* (PV), i.e. the interaction point related to the hard scattering of the event. All the other vertices are assumed to result from minimum bias interaction and are called *pile-up* vertices. In data recorded during 2012, an averange of

21 multiple interaction are occurred per bunch crossing, such a high vertex multiplicity strongly affects the ambient energy density in the event, a correct pile-up description is then crucial for MC simulation. The ATLAS MC production assures that events are simulated with various pile-up conditions, simulated events are then weighted according to the averange interaction per bunch crossing recorded in data.

1.2 Jets Reconstruction and Energy Calibration

Jets are reconstructed in ATLAS by means of the FastJet package [54], which provides a broad range of jet finding algorithms and analysis tools. In the following jet reconstruction methods relevant for the analysis presented in this theses are brifly described, for more detail see [53].

In general, jets may be reconstructed out of any set of four vector objects, however in ATLAS, the most important detectors for jet reconstruction are the ATLAS calorimeters. Calorimeter cells are grouped togheter by a clustering algorithm forming what are called *topological clusters* [55], those are three-dimensional cluster representing the energy deposition of the shower. the clustering starts with seed cells with a signal-to-noise ratio greather that a certain threshold, all nearby cells are grouped to the seed cells if they passes a second, lower, signal-to-noise ratio treshould.

Topological clusters are then fed to an *anti-k_t* algorithm [64]. The algorithm defines a metric to assess distances between the clusters i and j, the metric is defined as follows:

$$d_{ij} = \min(\frac{1}{k_{t,i}^2}, \frac{1}{k_{t,j}^2}) \cdot \frac{\Delta R_{ij}^2}{R^2} \tag{1.1}$$

$$d_i = \frac{1}{k_{t,i}^2} \tag{1.2}$$

where $k_{t,i}$ is the P_T of the cluster i and $\Delta R_{ij}^2 = \sqrt{\Delta\phi_{ij}^2 + \Delta\eta_{ij}^2}$, for this analysis $R = 0.4$ is chosen. If the distance between two cluster d_{ij} is smaller that d_i the clusters are grouped togheter and their four momentum summed, otherwise their are kept as single entity. The clustering procedure is iterated until is not possible to merge object anymore. The metric is designed in a way that high P_T jet will accumulate the soft activity surrounding them leading to conical jet shapes.

Given the high pile-up environment of LHC is important to distinguish jets coming from the hard scattering process and those related to pile-up interaction, for this purpose a techique, called *jet vertex fraction* (JVF), is implemented in the ATLAS jet reconstruction software. The JVF relies on Inner Detector informations, it is defined as the P_T weighted fraction of tracks pointing to to the primary vertex associated to the jet:

$$\text{JVF} = \frac{\sum\limits_{PV-tracks} P_T}{\sum\limits_{tracks} P_T} \tag{1.3}$$

the jet vertex fraction is only available within Inner Detector coverage $|\eta| < 2.5$, while calorimeter jet reconstruction is possible up to $|\eta| < 4.5$.

Calorimeter Jet Energy Calibration The ATLAS calorimeters were calibrated using test beam electrons [56], however the response to electromagnetic shower is different from the one to hadronic shower, a dedicated jet energy scale (JES) calibration is then performed by means of MC simulation [57]: jet energy is corrected to correspond, as a mean value, to the simulated energy of the hadronizing parton origin of the jet. The direction of the jet is also corrected to constraint it to point to the primary vertex instead to the center of the ATLAS detector. A set of corrections are then evaluated to take into account effect of pile-up [58, 59]. Jet resolution is also corrected in MC to better describe the data [60]. Finally, several jet energy scale correction are applied for a better agreement between data and simulation, those corrections are evaluated based on 2011 ATLAS data compared to MC simulation and exploits several techniques, JES systematic uncertainty due not perfect MC modeling are also evaluated, a full description of JES "in-situ" methodology corrections and related systematics uncertainties are described in [57, 61].

1.3 Jet b-Tagging

Typical decay lenght of b-hadron at ATLAS is of the order of few millimeter, exploiting the high precision of the Inner Detector tracker is possible to identify jet originatig from b-quarks with respect to other flavors, those jets are called *b-jets* and the identification technique used *b-tagging*.

Several algorithm has been developed in ATLAS for jet b-tagging, the relevant b-tagging algorithm to this thesis are briefly described in what follows, for more detailed description see [53]. The first step of jet b-tagging is to associate tracks to jets based on a ΔR cone matching, those tracks should satisfy strict selection criteria aimed to assure good quality and to reject tracks likely to come from strange hadron decays or photon conversion. For the discrimination between b-jet or light-jet (and in some cases also c-jet) algorithms uses the MC prediction of the distribution of some discriminating variable for the two hypotesis. Given the relatively high mass of b-hadrons, the tracks associated with b-jet will have spreaded impact parameters, this feature is used by the IP3D b-jet tagging algorithm, in which is implemented a discriminatig variable based on the sum of the impact parameter significances of all the tracks associated to the jet. An alternative approach, used by the $SV1$ algorithm, is instead to searches for inclusive secondary vertex formed by the decay products of the b-hadron, the search includes also the subsequent charm hadron decays. Another algorithm, called JetFitter [65], uses instead the direction of the jet to fully reconstruct the decay chain of b-hadron, the assuption made is that the decayed particles will lie along the jet axis. Finally, the three algorithm just described are combined togheter using an artificial neural network to maximize the discriminating power, the output of this neural network is referred as $MV1$ and is used in the search presented in this thesis.

The perfomance of the mentioned algorithms are evaluated in data and compared to simulation in [66]. B-hadron tagging efficiency and mistagging rate are the most common feature that describes the performance of a b-tagging algorithm, Figure 1.1

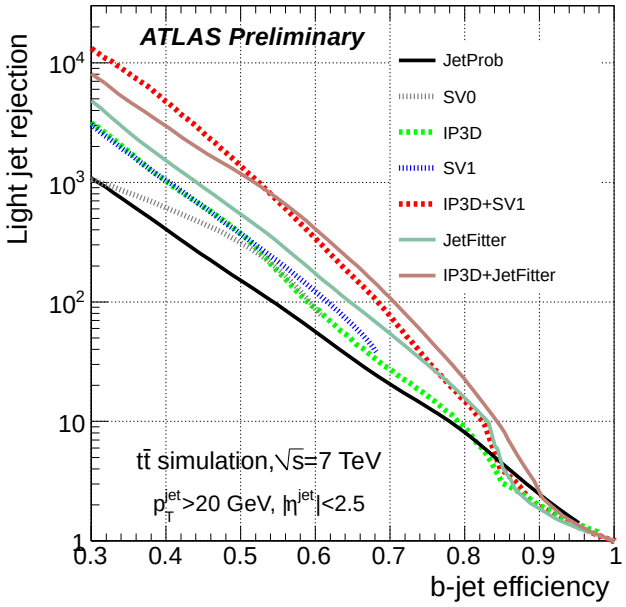

Figure 1.1: Light-jet rejection as a function of the b-jet tagging efficiency for different tagging algorithms [66]. Rejection here is defined as the inverse of mistagging rate, and the distributions are referred to a $t\bar{t}$ sample.

shows the b-tagging efficiency as a fuction of the inverse of the mistagging rate for different b-tagging algorithm, the tagging efficiency $\epsilon_b^{t\bar{t}}$ is usually referred to b-hadron in $t\bar{t}$ events and totally specify a b-tagging selection point. Correction due to non perfect modeling of b-tagging performance are evaluated by means of several methods for 2012 data in [84, 85] and used as event weights in MC simulation.

1.4 Electrons Reconstruction

Electron are reconstructed combining calorimeter and Inner Detector information, the ATLAS dedicated electron reconstruction algorithm is presented in [67]. The electron reconstruction starts from clusters of calorimeter cells, tracks are sought in the Inner Detector to match the cluster, special care is taken in order to account for Bremsstrahlung losses during the track matching stage. Once an electromagnetic shower in the calorimeter is found to match with one or more tracks, the combination is considered as an electron candidate. The energy is computed as a weighted average between the cluster energy and the track momentum, several corrections are applied to take into account energy loss in the material of the Inner Detector and effect of electromagnetic shower leakage. The ϕ and η directions are taken from the corresponding track parameters.

Further selection are applied to the electrons candidates to reduce contamination from pothon conversion and hadronic jet, there are three different identification criteria:

- Loose: selections related to the shape of the shower and to hadronic leackage are applied.

- Medium: additionally to the loose requirements, information on the strip layer of the electromagnetic calorimeter is used, stricter track matching requirements are also applied.

- Tight: additionally to medium requirements, converted photons are rejected by requiring a hit in the Inner Detector b-layer (if the module is expected to be operating), TRT electron identification capability is employed.

The electron identification performaces are compared between data and simulation in [68], correction to the electron identification efficiency are estimated and applied as weight to simulated electron candidates. Additional corrections are applied to the energy scale and resolution of simulated electron to match the one in data according to [69]. Finally, the electrons usend in the presented analysis are rejected if matching with a region of the calorimeter with readout problems or suffering from high noise.

Prompt electrons, coming from the decay of a resonance like the Z^0 boson or the Higgs boson are very likely to be *isolated*, i.e. very little activity is expected in their sourraundings, this is in contrast to electron that come from decay of hadrons, which instead will be likely to be embedded in a jet of particle. Two isolation variables are then defined by the sum of the energy in a ΔR cone around the electron candidate:

- Track isolation P_T^{cone}: which is the scalar sum of the track P_T in a $\Delta R \leq 0.4$ cone around the electron, the electron track is not considered.

- Calorimeter isolation E_T^{cone}: which is the scalar sum of topological cluster transverse energy in a $\Delta R \leq 0.2$ cone around the electron. Cluster associated to the electron are not considered. This variable is corrected as a function of the vertex multiplicity in the event in order to assure a constant selection efficiency.

1.5 Muons Reconstruction

ATLAS employs a variety of strategies for identifying and reconstructing muons, the main detector used for this purpose is the Muon Spectrometer, which may be supplemented with others detectors informations. A detailed description of the muon reconstruction algorithms and their performance is reported in [53], in the following only the muon reconstruction strategy relevant for this thesis is described.

The STACO *combined* muon algorithm [70] associate tracks found in the Muon Spectrometer with the corresponding Inner Detector track and calorimeter information, the muons are then identified at their production vertex with optimum parameter resolution. First track segment are reconstructed in each of the three muon station, segments are then liked togheter to form a track. The muon track is extrapolated to the Inner Detector taking into account energy loss and multiple scattering in the calorimeters, then, it is matched with a Inner Detector track via

χ^2 matching. Finally a statistical combination of the Inner Detector and Muon Spectrometer tracks is performed to obtain a combined vector.

Muon reconstruction efficiency, momentum scale and resolution are evaluated in [71], performance are compared with MC simulation and a set of corrections, aimed to restore agreement between data and simulation, are provided. Correction on muon momentum scale, resolution and reconstruction efficiency are applied to muons in the presented analysis.

Isolation variable, as described for electrons, are also implemented for muons, with the only exception of the use of calorimeter cluster with fixed size in the definition of E_T^{cone}. Similar pile-up corrections are also used for muons.

1.5.1 b-Tagging

The tagging of jets due to the hadronisation of b-quarks is performed using the MV1 b-tagging algorithm [**?**]. This neural network based algorithm uses the output weights of the JetFitter+IP3D, IP3D and SV1 b-taggers as inputs. The working point that gives a nominal b-tagging efficiency of 70% on $t\bar{t}$ samples is used.

1.5.2 Taus

Hadronically decaying tau candidates are reconstructed using clusters in both the electromagnetic and hadronic calorimeters. A preselection is applied to the candidates that requires the reconstructed τ candidates to have a transverse momentum of $P_T > 20$GeV and to have a reconstructed pseudorapidity of $|\eta| < 2.5$. Furthermore, it is required that the candidates have either one or three tracks within a cone of $\Delta R < 0.2$ associated to them and have a charge of ± 1. Finally, the preselected tau candidates should pass the BDT-Medium multivariant tau identification selection as well as the dedicated electron and muon vetoes for hadronically decaying tau candidates.

1.5.3 Overlap Removal

After the preselection of the physics objects needed for this analysis, an overlap removal between the different objects is then applied to avoid double-counting. The distance between two objects in rapidity $\Delta\eta$ and polar angle $\Delta\phi$ is defined as $\Delta R = \sqrt{(\Delta\eta)^2 + (\Delta\phi)^2}$. Overlap removal is then applied in the following order:

- preselected electrons are removed if they overlap with a preselected muon within $\Delta R < 0.2$,
- preselected taus are removed if they overlap with a preselected muon or electron within $\Delta R < 0.2$,
- preselected jets are removed if they overlap with a preselected muon, electron or tau within $\Delta R < 0.2$.

1.5.4 Missing Transverse Energy

The missing transverse energy, E_T^{miss}, is calculated using the RefFinal method, which takes the energy deposited in the calorimeter, the muons reconstructed in the muon spectrometer and tracks reconstructed in the inner detector as inputs. For this, the energy deposits are calibrated based upon the high-*pt* physics object they are associated to, with an order of preference of electrons, photons, hadronically decaying taus, jets and finally muons. Any unassociated energy deposits are combined into the so-called "soft-term". To reduce the effect of pileup on the E_T^{miss} calculation, corrections are applied to both the jets in an event and to the soft-term. Firstly, any jet with a pseudorapidity of $|\eta| < 2.4$ that enters the E_T^{miss} calculation is weighted by it's JVF. Similarly, the soft-term is weighted by the soft-term-vertex-fraction (STVF) of the event - the ratio given by

$$STVF = \frac{\sum_{track,PV} P_T}{\sum_{track} P_T} \tag{1.4}$$

where $\sum_{track,PV} P_T$ is the sum of the transverse momentum of all tracks in the event associated to the primary vertex, but unmatched to physics objects, and $\sum_{track} P_T$ is the sum of the transverse momentum of all tracks in the event unmatched to physics objects. Any calibration applied to the energy or direction of the physics objects in the final analysis is also propagated to the E_T^{miss}.

1.5.5 Vertices

In this analysis vertices are selected that have a minimum of three associated tracks: this helps to ensure that the selected vertices come from beam-beam interactions rather than, for instance, cosmic muons.

1.5.6 Event Cleaning

In addition to the data quality requirements described in section **??**, further selections are applied to veto events where bad jets are identified as arising from detector effects (coherent noise in the EM and Tile calorimeters or spikes in the HEC calorimeter), cosmics or beam based background. To reject events, the recommendations of the JetEtMiss performance group [**?**] are followed: Events are rejected if at least one AntiKt4LCTopo jet with $p_T > 20$GeV, that passes the overlap removal with electrons, muons and taus described in section 1.5.3, fails the `BadLooseMinus` selection or points towards the hot Tile Calorimeter cells identified in data taking periods B1 and B2 [**?**].

1.5.7 Monte Carlo Corrections

The MC samples used on this analysis are corrected to account for differences between the simulation and data in the trigger, lepton reconstruction and identification and b-tagging efficiencies. Furthermore, the MC is reweighted so that the vertex multiplicity distribution agrees with that in the data.

Physics Object	Preselection
Electrons	$P_T > 15$GeV
	$\|\eta\| < 1.37$ or $1.52 < \|\eta\| < 2.47$
	`Medium++`
	Author = 1 or 3
	Pass Object Quality Flag
Muons	$P_T > 10$GeV
	$\|\eta\| < 2.5$
	isLoose STACO muon
	Inner Detector track quality requirements
	Inner Detector track $\|z_0^{PV}\| < 10$mm
Jets	$P_T > 30$GeV
	$\|\eta\| < 4.5$
	$\|JVF\| > 0.5$ for jets with $\|\eta\| < 2.4$ and $P_T < 50$GeV
Jets (taggable)	$P_T > 20$GeV
	$\|\eta\| < 2.5$
	$\|JVF\| > 0.5$ for jets with $\|\eta\| < 2.4$ and $P_T < 50$GeV
Taus	$P_T > 20$GeV
	$\|\eta\| < 2.5$
	BDT Medium
	$N_{tracks} =$ 1 or 3
	Author = 1 or 3
	Muon and Electron Veto
E_T^{miss}	RefFinal with STVF correction
Vertices	$N_{tracks} \geq 3$

Table 1.1: Summary of the preselections used for physics objects in this analysis

Trigger Efficiency corrections

Correction factors are applied to the simulated trigger efficiency for both the single electron,
`EF_e24vhi_medium1`, and combined electron-muon, `EF_e12Tvh_medium1_mu8`, triggers used in this analysis. The trigger efficiency for the `EF_e24vhi_medium1` has been measured with respect to offline electrons using a tag and probe method in $Z \to ee$ events [**?**]. Scale factors are derived from the ratio of the trigger efficiency measured in data and MC, measured as a function of electron P_T and η.

For the `EF_e12Tvh_medium1_mu8` trigger, correction factors are measured separately for the two individual legs of the trigger, `EF_e12Tvh_medium1` and `EF_mu8` [**?**]. The product of the two correction factors is then used as the overall scaling factor. The trigger efficiency for the `EF_e12Tvh_medium1` leg has been measured with respect to offline electrons using a tag and probe method for $Z \to ee$ events in both data and MC. Likewise, the `EF_mu8` trigger efficiency scale factors are derived using a tag and probe measurement with $Z \to \mu\mu$ events. Oncemore, scale factors are derived from the ratio of the trigger efficiency measured in data and MC, measured as a function of electron P_T and η.

Lepton Reconstruction Efficiency Corrections

Further correction factors are applied to the MC samples to account for differences in the lepton reconstruction and identification efficiencies between data and simulation. Scale factors for the electron identification and reconstruction efficiencies are measured separately using a combination of $Z \to ee$ and $J/\psi \to ee$ tag and probe measurements [**?**]. Both sets of scale factors are measured as a function of the electron E_T and η.

Similarly, muon reconstruction efficiency scale factors have been measured, using a $Z \to \mu\mu$ tag and probe analysis, as a function of the muon P_T, η, ϕ and charge [**?**].

b-tagging Efficiency Corrections

Corrections are applied to the b-tagging efficiency and mistag rate in MC, using a combination of the System8 and likelihood scale factor measurements [84]. Separate scale factors are applied, as a function of the jet P_T and η, based on the origin of the jet at truth level - ie. depending on if the jet originates from a b quark, a c quark, a τ lepton or a light quark.

Pileup Reweighting

Differences between the distribution of the average number of interactions per bunch crossing, $< \mu >$, in MC and data are corrected by reweighting the MC $< \mu >$ distribution to that in the full considered dataset. An additional scaling of $1.1\times <$ $\mu >$ is applied to the MC, which has been shown to improve the description of the number of primary vertices distribution of the data.

Bibliography

[1] L. Evans and P. Bryant, *LHC Machine*, JINST **3** (2008) S08001.

[2] F. Englert and R. Brout, *Broken Symmetry and the Mass of Gauge Vector Mesons*, Phys. Rev. Lett. **13** (1964) 321.

[3] P. W. Higgs, *Broken symmetries, massless particles and gauge fields*, Phys. Lett. **12** (1964) 132.

[4] P. W. Higgs, *Broken Symmetries and the Masses of Gauge Bosons*, Phys. Rev. Lett. **13** (1964) 508.

[5] P. W. Higgs, *Spontaneous Symmetry Breakdown without Massless Bosons*, Phys. Rev. **145** (1966) 1156.

[6] G. S. Guralnik, C.R. Hagen and T. W. B. Kibble Phys.Rev.Lett. **13** (1964) 585.

[7] N. P. Nilles, *Supersymmetry, supergravity and particle physics*, Phys. Rep. **110** (1984) 1.

[8] H. E. Haber and G. L. Kane, *The search for supersymmetry: Probing physics beyond the standard model*, Phys. Rep. **117** (1985) 75.

[9] ALEPH, DELPHI, L3 and OPAL Collaboration, *Search for neutral MSSM Higgs bosons at LEP*, Eur. Phys. J. **C47** (2006) 547.

[10] *Combined CDF and D0 upper limits on MSSM Higgs boson production in tau-tau final states with up to 2.2 fb^{-1} of data*, `arXiv:1003.3363 [hep-ex]`.

[11] CDF Collaboration, T. Aaltonen et al. Phys. Rev. Lett. **103** (2009) 201801.

[12] D0 Collaboration, V. Abazov et al. Phys. Rev. Lett. **101** (2008) 071804.

[13] TNPWG (Tevatron New Physics Higgs Working Group), CDF and D0 Collaborations, *Search for Neutral Higgs Bosons in Events with Multiple Bottom Quarks at the Tevatron*, `arXiv:1207.2757 [hep-ex]`.

[14] CDF Collaboration, T. Aaltonen et al., *Search for Higgs Bosons Produced in Association with b-quarks*, Phys.Rev. **D85** (2012) 032005, `arXiv:1106.4782 [hep-ex]`.

[15] D0 Collaboration, V.M. Abazov et al., *Search for neutral Higgs bosons in the multi-b-jet topology in 5.2fb^{-1} of $p\bar{p}$ collisions at $\sqrt{s} = 1.96$ TeV*, Phys.Lett. **B698** (2011) 97–104, arXiv:1011.1931 [hep-ex].

[16] The CMS Collaboration, S. Chatrchyan et al., arXiv:1104.1619 [hep-ex] [hep-ex].

[17] The ATLAS Collaboration , *Search for the neutral Higgs bosons of the Minimal Supersymmetric Standard Model in pp collisions at $\sqrt{s} = 7$ TeV with the ATLAS detector*, arXiv:1211.6956 [hep-ex].

[18] T. A. Collaboration, *Observation of a new particle in the search for the Standard Model Higgs boson with the ATLAS detector at the LHC*, Physics Letters B **716** (2012) 1–29.

[19] T. C. Collatoration, *Observation of a new boson at a mass of 125 GeV with the CMS experiment at the LHC*, Physics Letters B **716** (2012) 30–61.

[20] S. Heinemeyer, O. Stål and G. Weiglein, *Interpreting the LHC Higgs search results in the MSSM*, Phys.Lett. **B710** (2012) 201–206, arXiv:1112.3026 [hep-ph].

[21] A. Arbey, M. Battaglia, A. Djouadi and F. Mahmoudi, *The Higgs sector of the phenomenological MSSM in the light of the Higgs boson discovery*, JHEP **1209** (2012) 107, arXiv:1207.1348 [hep-ph].

[22] The ATLAS Collaboration, G. Aad et al., *The ATLAS Experiment at the CERN Large Hadron Collider*, JINST **3** (2008) S08003.

[23] M. L. Mangano et al., *ALPGEN, a generator for hard multiparton processes in hadronic collisions*, JHEP **07** (2003) 001.

[24] J. Alwall et al., *Comparative study of various algorithms for the merging of parton showers and matrix elements in hadronic collisions*, Eur. Phys. J. **C53** (2008) 473, arXiv:0706.2569.

[25] S. Frixione and B. R. Webber, *Matching NLO QCD computations and parton shower simulations*, JHEP **06** (2002) 029, hep-ph/0204244.

[26] B. P. Kersevan and E. Richter-Was, *The Monte Carlo Event Generator AcerMC 2.0 with Interfaces to PYTHIA 6.2 and HERWIG 6.5*, arXiv:0405247v1 [hep-ph].

[27] G. Corcella et al., *HERWIG 6: an event generator for hadron emission reactions with interfering gluons (including supersymmetric processes)*, JHEP **01** (2001) 010.

[28] J. M. Butterworth, J. R. Forshaw, and M. H. Seymour, *Multiparton Interactions in Photoproduction at HERA*, Z. Phys. **C72** (1996) 637.

[29] T. Binoth, M. Ciccolini, N. Kauer, and M. Kramer, *Gluon-induced W-boson pair production at the LHC*, JHEP **12** (2006) 046.

[30] A. S. et al., *Higgs boson production in gluon fusion*, JHEP **02** (2009) 029.

[31] T. Gleisberg et al., *Event generation with SHERPA 1.1*, JHEP **02** (2009) 007.

[32] J. Pumplin, D. R. Stump, J. Huston, H. L. Lai, P. M. Nadolsky and W. K. Tung, "New generation of parton distributions with uncertainties from global QCD analysis," JHEP **0207** (2002) 012 [hep-ph/0201195].

[33] H. -L. Lai, M. Guzzi, J. Huston, Z. Li, P. M. Nadolsky, J. Pumplin and C. -P. Yuan, "New parton distributions for collider physics," Phys. Rev. D **82** (2010) 074024 [arXiv:1007.2241 [hep-ph]].

[34] S. Heinemeyer *et al.* [LHC Higgs Cross Section Working Group Collaboration], "Handbook of LHC Higgs Cross Sections: 3. Higgs Properties," arXiv:1307.1347 [hep-ph].

[35] M. Carena, S. Heinemeyer, C. E. M. Wagner, and G. Weiglein, *Suggestions for benchmark scenarios for MSSM Higgs boson searches at hadron colliders*, Eur. Phys. J. **C26** (2003) 601–607, `hep-ph/0202167`.

[36] The ATLAS Collaboration, *ATLAS Monte Carlo Tunes for MC09*, ATL-PHYS-PUB-2010-002.

[37] S. Jadach, J. H. Kuhn and Z. Was, *TAUOLA - a library of Monte Carlo programs to simulate decays of polarized τ leptons*, Comput. Phys. Commun. **64** (1990) 275.

[38] E. Barberio, B. V. Eijk and Z. Was, *Photos - a universal Monte Carlo for QED radiative corrections in decays*, Comput. Phys. Commun. **66** (1991) 115.

[39] The GEANT4 Collaboration, S. Agostinelli et al., *GEANT4 - a simulation toolkit*, Nucl. Instrum. Meth. **A506** (2003) 250.

[40] The ATLAS Collaboration, G. Aad et al., *The ATLAS Simulation Infrastructure*, ATLAS-SOFT-2010-01-004, submitted to Eur. Phys. J. C., `arXiv:1005.4568`.

[41] The ATLAS Collaboration, *Estimation of $Z \to \tau\tau$ Background in VBF $H \to \tau\tau$ Searches from $Z \to \mu\mu$ Data using an Embedding Technique*, ATL-PHYS-INT-2009-109.

[42] The ATLAS Collaboration, *Search for the Standard Model Higgs boson in the $H \to \tau\tau$ decay mode with 4.7 f b1 of ATLAS detactor*, Tech. Rep. ATLAS-CONF-2012-014, CERN, Geneva, Mar, 2012.

[43] The ATLAS Collaboration, *Search for the Standard Model Higgs boson $H \to \tau\tau$ decays with the ATLAS detector*, ATL-COM-PHYS-2013-722.

[44] T. S. et al., Z *physics at LEP 1*, CERN 89-08 **3** (1989) 143.

[45] A. Bazan, T. Bouedo, P. Ghez, M. Marino and C. Tull, "The Athena data dictionary and description language," eConf C **0303241** (2003) MOJT010 [cs/0305049 [cs-se]].

[46] The ATLAS Collaboration, Inner Detector: Technical Design Report, CERN/LHCC/97-016/017 (1997).

[47] The ATLAS Collaboration, G. Aad et al., The ATLAS Experiment at the CERN Large Hardon Collider, 2008 JINST 3 S08003.

[48] T. Cornelissen et al., Concepts, Design and Implementation of the ATLAS New Tracking, ATLAS Note ATL-SOFT-PUB-2007-007 (2007).

[49] Kalman, R. E. (1960). *"A New Approach to Linear Filtering and Prediction Problems".* Journal of Basic Engineering 82 (1): 3545. doi:10.1115/1.3662552

[50] The ATLAS Collaboration, *Characterization of Interaction-Point Beam Parameters Using the pp Event-Vertex Distribution Reconstructed in the ATLAS Detector at the LHC*, ATL-CONF-2010-027.

[51] R. Fruhwirth, W. Waltenberger, P. Vanlaer, *Adaptive vertex fitting*, J. Phys. G34 (2007).

[52] The ATLAS Collaboration, Performance of primary vertex reconstruction in proton-proton collisions at $s = sqrt(7)$ TeV in the ATLAS experiment. ATLAS-CONF-2010-069.

[53] The ATLAS Collaboration, *Expected Performance of the ATLAS Experiment - Detector, Trigger and Physics*, CERN-OPEN-2008-020, `arXiv:0901.0512`.

[54] M. Cacciari, G. P. Salam, and G. Soyez, *FastJet user manual*, Eur.Phys.J. C72 (2012) 1896.

[55] W. Lampl et al., *Calorimeter Clustering Algorithms : Description and Performance*, ATL-LARG-PUB-2008-002.

[56] E. Abat, J. Abdallah, T. Addy, P. Adragna, et al., *Combined performance studies for electrons at the 2004 ATLAS combined test-beam*, JINST 5 (2010) P11006.

[57] ATLAS Collaboration, *Jet energy measurement with the ATLAS detector in proton-proton collisions at* $\sqrt{s} = 7$ *TeV*, Submitted to EPJ (2011) , arXiv:1112.6426

[58] The ATLAS Collaboration, *Pile-up corrections for jets from proton-proton collisions at ATLAS in 2011*, ATLAS-CONF-2012-064, July, 2012.

[59] M. Cacciari and G. P. Salam, *Pileup subtraction using jet areas*, Phys.Lett. B659 (2008) 119.

[60] The ATLAS Collaboration, G. Aad et al., *Jet energy resolution in proton-proton collisions at $\sqrt{s} = 7$ TeV recorded in 2010 with the ATLAS detector*, Eur.Phys.J. C73 (2013) 2306

[61] The ATLAS collaboration, *Jet energy scale and its systematic uncertainty in proton-proton collisions at $\sqrt{s} = 7$ TeV with ATLAS 2011 data*, ATLAS-CONF-2013-004

[62] T. Barillari et al., *Local Hadron Calibration*, ATL-LARG-PUB-2009-001.

[63] The ATLAS Collaboration, *Jet energy scale and its systematic uncertainty in proton-proton collisions at $\sqrt{s} = 7$ TeV in ATLAS 2010 data*, ATLAS-CONF-2011-032.

[64] M. Cacciari, G. P. Salam, and G. Soyez, *The anti-kt jet clustering algorithm*, JHEP 04 (2008) 63.

[65] G. Piacquadio, C. Weiser, *A new inclusive secondary vertex algorithm for b-jet tagging in ATLAS*, JPCS 119 (2008) 032032

[66] The ATLAS Collaboration, G. Aad et al., *Commissioning of the ATLAS high-performance b-tagging algorithms in the 7 TeV collision data, ATLAS-CONF-2011-102*, CERN, 2011, ATLAS-CONF-2011-102.

[67] The ATLAS collaboration, *Expected electron performance in the ATLAS experiment*, ATL-PHYS-PUB-2011-006

[68] The ATLAS Collaboration, *Electron reconstruction and identification efficiency measurements with the ATLAS detector using the 2011 LHC proton-proton collision data*, CERN-PH-EP-2014-040, arXiv:1404.2240

[69] The ATLAS Collaboration, G. Aad et al., *Electron performance measurements with the ATLAS detector using the 2010 LHC proton-proton collision data*, Eur.Phys.J. C72 (2012) 1909.

[70] S. Hassini, et al., *A muon identification and combined reconstruction procedure for the ATLAS detector at the LHC using the (MUONBOY, STACO, MuTag) reconstruction packages*, NIM A572 (2007) 7779.

[71] The ATLAS Collaboration, G. Aad et al., *Preliminary results on the muon reconstruction efficiency, momentum resolution, and momentum scale in ATLAS 2012 pp collision data*, ATLAS-CONF-2013-088, CERN, 2013,

[72] The ATLAS Collaboration, *Reconstruction and Calibration of Missing Transverse Energy and Performance in Z and W events in ATLAS Proton-Proton Collisions at $\sqrt{s}$=7 TeV*, ATLAS-CONF-2011-080.

[73] TheATLAS Collaboration, *Performance of the Reconstruction and Identification of Hadronic tau Decays in ATLAS with 2011 Data*, ATLAS-CONF-2012-142.

[74] A. Elagin, P. Murat, A. Pranko, and A. Safonov, *A New Mass Reconstruction Technique for Resonances Decaying to di-tau*, arXiv:1012.4686 [hep-ex]. * Temporary entry *.

[75] ATLAS Jet/EtMiss Combined Performance Group, *Jet Energy Resolution Provider*, https://twiki.cern.ch/twiki/bin/view/Main/JetEnergyResolutionProvider.

[76] The ATLAS Collaboration, *Data-Quality Requirements and Event Cleaning for Jets and Missing Transverse Energy Reconstruction with the ATLAS Detector in Proton-Proton Collisions at a Center-of-Mass Energy of $\sqrt{s} = 7$ TeV*, ATLAS-CONF-2010-038.

[77] T. A. Collaboration, *Search for neutral MSSM Higgs bosons decaying to $\tau\tau$ pairs in proton-proton collisions at with the ATLAS detector*, Physics Letters B **705** (2011) no. 3, 174 – 192.

[78] The ATLAS Collaboration, *Data-driven estimation of the background to charged Higgs boson searches using hadronically-decaying tau final states in ATLAS,* ATLAS-CONF-2011-051.

[79] The ATLAS Collaboration, *Measurement of the $Z \to \tau\tau$ cross section with the ATLAS detector*, Phys. Rev. D **84** (2011) 112006.

[80] T. A. Collaboration, *Search for the neutral Higgs bosons of the Minimal Supersymmetric Standard Model in pp collisions at $\sqrt{s} = 7$ TeV with the ATLAS detector*, JHEP , arXiv:1211.6956.

[81] Atlas statistics forum, *ABCD method in searches*, link

[82] The ATLAS Collaboration, *Search for Neutral MSSM Higgs Bosons H to $\tau\tau$ to $l\tau_h$ with the ATLAS Detector in 7 TeV Collisions*, ATL-COM-PHYS-2012-094.

[83] The ATLAS Collaboration, *Search for neutral Higgs Bosons in the decay mode $H \to \tau\tau \to ll{+}4\nu$ in proton proton collision at $\sqrt{7}$ TeV with the ATLAS Detector*, ATL-COM-PHYS-2011-758.

[84] The ATLAS Collaboration, *Measuring the b-tag efficiency in a ttbar sample with 4.7 fb^{-1} of data from the ATLAS detector* ATLAS-CONF-2012-097.

[85] The ATLAS Collaboration, *Calibration of b-tagging using dileptonic top pair events in a combinatorial likelihood approach with the ATLAS experiment* ATLAS-CONF-2014-004.

[86] The ATLAS Collaboration, *Luminosity Determination in pp Collisions at $\sqrt{s} = 7$ TeV using the ATLAS Detector in 2011*, ATLAS-CONF-2011-116.

[87] T. Sjostrand, S. Mrenna and P. Skands, *PYTHIA 6.4 physics and manual*, JHEP **05** (2006) 026.

[88] A. B. et al., *Rivet user manual*, arXiv:1003.0694 [hep-ph].

[89] E. G. G. Cowan, K. Cranmer and O. Vitells, *Asymptotic formulae for likelihood-based tests of new physics*, `arXiv:1007.1727 [hep-ex]`.

[90] LHC Higgs Cross Section Working Group, S. Dittmaier, C. Mariotti, G. Passarino, R. Tanaka (Eds.), et al., *Handbook of LHC Higgs Cross Sections: 1. Inclusive Observables*, `arXiv:1101.0593 [hep-ph]`.

[91] LHC Higgs Cross Section Working Group, S. Dittmaier, C. Mariotti, G. Passarino, and R. Tanaka (Eds.), *Handbook of LHC Higgs Cross Sections: 2. Differential Distributions*, CERN-2012-002 (CERN, Geneva, 2012) , `arXiv:1201.3084 [hep-ph]`.

[92] ATLAS collaboration *Performance of the ATLAS Silicon Pattern Recognition Algorithm in Data and Simulation at* $\sqrt{s} = 7$ *TeV*, ATLAS-CONF-2010-072

[93] The ATLAS Collaboration, *A measurement of the material in the ATLAS inner detector using secondary hadronic interactions*, arXiv:1110.6191, JINST 7 (2012) P01013

[94] The ATLAS Collaboration, *Validation of the ATLAS jet energy scale uncertainties using tracks in proton-proton collision* $\sqrt{s} = 7$ *TeV*, ATLAS-CONF-2011-067

[95] The ATLAS Collaboration, *Track Reconstruction Efficiency in* $\sqrt{s} = 7$ *TeV Data for Tracks with* $P_T > 100$ *MeV* , ATL-PHYS-INT-2010-112

[96] D. de Florian, G. Ferrera, M. Grazzini and D. Tommasini, *Transverse-momentum resummation: Higgs boson production at the Tevatron and the LHC*, JHEP **1111** (2011) , `arXiv:1109.2109 [hep-ph]`.

[97] Statistical twiki, NuissanceCheck. https://twiki.cern.ch/twiki/bin/view/AtlasProtected/Nuisan